ADVANCED OPTICAL MATERIALS

Supporting Information

for *Adv. Optical Mater.*, DOI: 10.1002/adom.201900739

Enhancing the Purity of Reflective Structural Colors with Ultrathin Bilayer Media as Effective Ideal Absorbers

*Zhengmei Yang, Chengang Ji, Dong Liu, and L. Jay Guo**

Supporting Information for

Enhancing the purity of reflective structural colors with ultra-thin bilayer media as effective ideal absorbers

Zhengmei Yang,[1, 2,#] Chengang Ji,[1,#] Dong Liu,[3] and L. Jay Guo[1,*]

[1] Department of Electrical Engineering and Computer Science, University of Michigan, Ann Arbor, Michigan 48109, USA

[2] School of Physics and Electronics, State Key Laboratory of Advanced Design and Manufacturing for Vehicle Body, Hunan University, Changsha 410082, China

[3] MIIT Key Laboratory of Thermal Control of Electronic Equipment, School of Energy and Power Engineering, Nanjing University of Science and Technology, Nanjing 210094, China.

[#] These authors contribute equally to this work.

* Corresponding author: guo@umich.edu

1. The thickness selection of the absorber layer

The absorber layer should be much thinner than the wavelength to avoid intrinsic absorption in this layer at λ_c, so the electric field intensity in this layer can be approximated to be constant. Resultantly, the electric field intensities at the 2-3 interface ($E(\mathrm{z} = d_4 + d)$) and the 3-4 interface ($E(\mathrm{z} = d_4)$) can both be approximated to zero since the absorber layer is placed at the position where $E(\lambda_c) \sim 0$ to achieve high reflectivity. Therefore, the reflection coefficients at these two interfaces should be close to -1 due to the coincidence of forward electric field and reflected electric field, that is:

$$r_{345} = \frac{r_{34} + r_{45} e^{2i\beta_4}}{1 + r_{34} r_{45} e^{2i\beta_4}} \to -1, \tag{1}$$

$$r_{2345} = \frac{r_{23} + r_{345} e^{2i\beta_3}}{1 + r_{23} r_{345} e^{2i\beta_3}} \to -1, \tag{2}$$

where $r_{pq} = \frac{m_p - m_q}{m_p + m_q}$, $m_p = n_p + ik_p$ is the complex refractive index of layer p, $\beta_4 = 2\pi n_4 d_4/\lambda_c$, $\beta_3 = 2\pi(n + ik)d/\lambda_c$. By substituting Equation (1) into Equation (2), we get

$$r_{2345} = \frac{r_{23} - e^{2i\beta_3}}{1 - r_{23} e^{2i\beta_3}} \to -1. \tag{3}$$

It yields

$$e^{2i\beta_3} = \exp\left(-\frac{4\pi k d}{\lambda_c}\right) * \exp\left(i\frac{4\pi n d}{\lambda_c}\right) \to 1, \tag{4}$$

which requires $\frac{4\pi n d}{\lambda_c} \to 2m\pi$ $(m = 0,1, \ldots)$. Considering the skin depths of common metals, $\frac{4\pi n d}{\lambda_c}$ should be close to 0, thus $d \ll \frac{\lambda_c}{4\pi n}$.

2. The design of high-purity red and green color filters

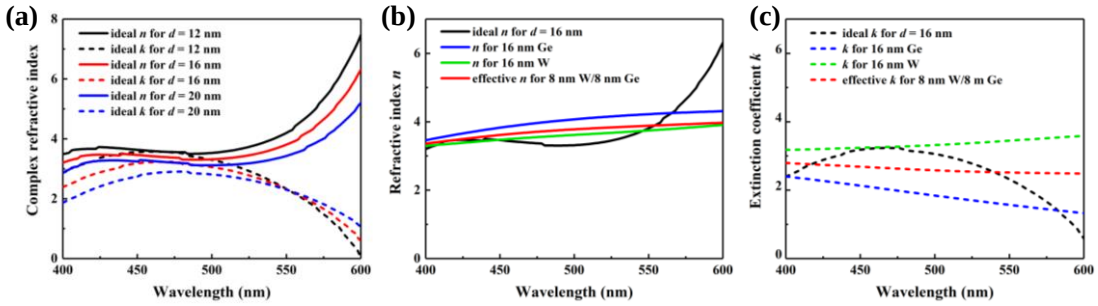

Figure S1. (a) The calculated ideal complex refractive indices (*n*, *k*) of the absorber layer in a wavelength range from 400 nm to 600 nm for producing highly pure red color filters when the thickness *d* is fixed to 12 nm, 16 nm and 20 nm, respectively. Comparisons of (b) the refractive indices and (c) extinction coefficients of the ideal absorber material, single lossy medium Ge, W and the W/Ge bilayer film in the case of *d* = 16 nm for the red color filter.

For high-purity red color filters, the thickness of the middle Ta_2O_5 layer is fixed at d_4 = 130 nm corresponding to the half-wave optical thickness of λ_c = 630 nm and the thickness of the top Ta_2O_5 layer is fixed at d_2 = 44 nm corresponding to the quarter-wave optical thickness of the target wavelength λ_0 = 400 nm, where the reflection gets suppressed. The wavelength region of zero reflectivity should be from 400 nm to 600 nm. Figure S1a plots the calculated ideal *n* and *k* at different wavelengths when the absorber layer thickness *d* is 12, 16 and 20 nm, respectively. The ideal *n* and *k* can be effectively adjusted by changing the thickness of the absorber layer. Besides, the values of the ideal *n* and *k* gradually decrease when increasing the thickness *d* from 12 to 20 nm. Figure S1b and Figure S1c compare the complex refractive indices of the ideal absorber material, single lossy medium germanium (Ge), tungsten (W) and the W/Ge bilayer film in the case of *d* = 16 nm. It is obvious that the effective (*n*, *k*) of the bilayer absorber comprised of 8 nm W and 8 nm Ge is closer to the ideal (*n*, *k*).

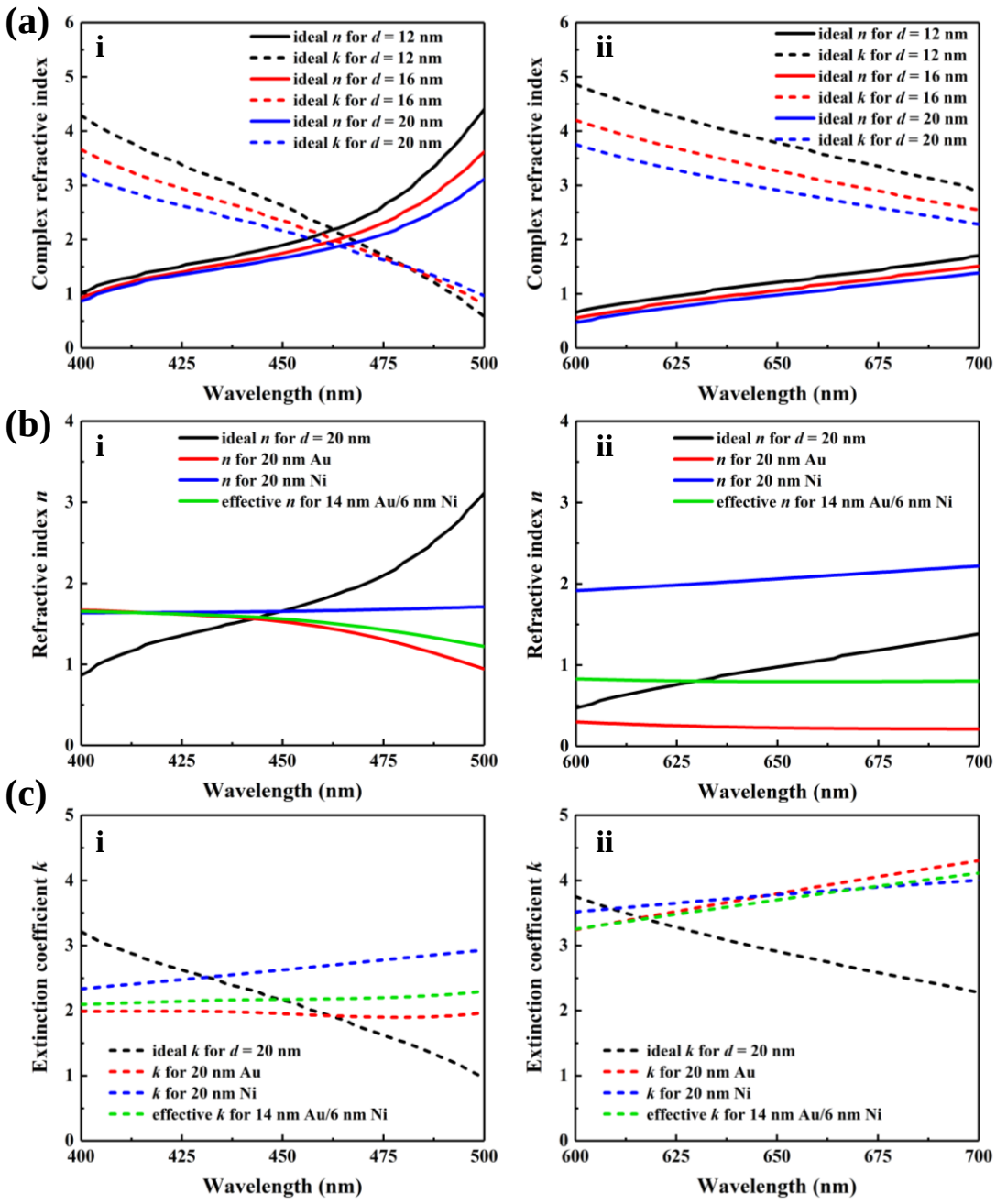

Figure S2. (a) The calculated ideal complex refractive indices (*n*, *k*) of the absorber layer in two wavelength regions (400 ~ 500 nm and 600 ~ 700 nm) for producing highly pure green color filters when the thickness *d* is fixed to 12 nm, 16 nm and 20 nm, respectively. Comparisons of (b) the refractive indices and (c) extinction coefficients of the ideal absorber material, single metal Au, Ni and the Au/Ni bilayer film in the case of *d* = 20 nm for the green color filter.

In order to obtain high-purity green color filters, zero reflectivity should be achieved in two wavelength ranges (400 ~ 500 nm and 600 ~ 700 nm) at the same time. The

thickness of the middle Ta_2O_5 layer is fixed at d_4 = 228 nm corresponding to one wavelength optical thickness of λ_c = 525 nm. At this thickness, a narrower reflection bandwidth can be created by the second-order F-P cavity resonance mode, resulting in better color purity. The thickness of the top Ta_2O_5 layer is fixed at d_2 = 26 nm corresponding to the one-eighth wavelength optical thickness of the target wavelength λ_0 = 460 nm, where the reflection gets suppressed. The much thinner thickness of the AR layer for the green color filter is resulted from the non-trivial reflection phase shift of ~ 0.5π occurring at the 2-3 interface at the wavelength of λ_0 (See more details at Figure S3). Figure S2a shows the calculated ideal *n* and *k* at different wavelengths when the absorber layer thickness *d* is 12, 16 and 20 nm, respectively. Obviously, the ideal (*n*, *k*) values in the short wavelength range and long wavelength range are quite different. Similar to that of blue and red color filters, the overall ideal (*n*, *k*) values also exhibit a decreasing trend as the absorber layer thickness *d* increases from 12 to 20 nm. Figure S2b and Figure S2c compare the complex refractive indices of the ideal absorber layer, single metal Au, Ni and the Au/Ni bilayer film in the case of *d* = 20 nm. It is apparent that the bilayer absorber comprised of 14 nm Au and 6 nm Ni provides a better match between their effective (*n*, *k*) and the ideal (*n*, *k*) in this two wavelength ranges.

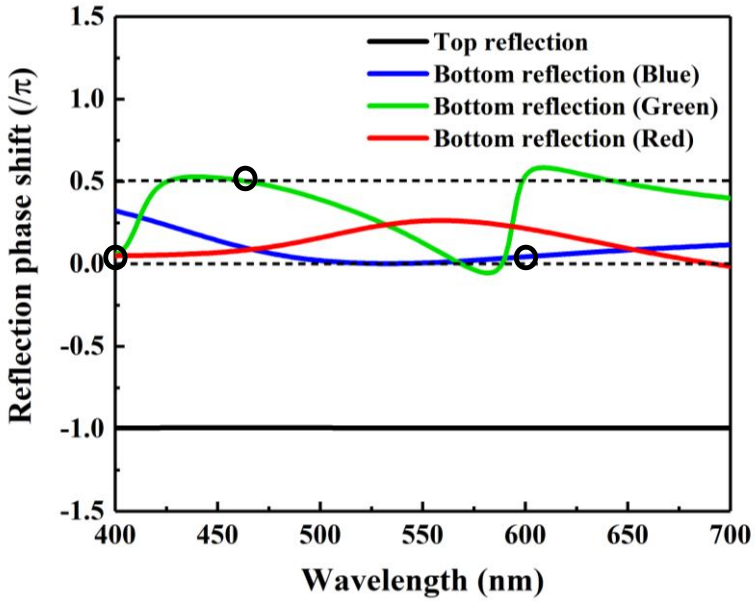

Figure S3. The top reflection phase shift (the black curve) and the bottom reflection phase shifts (the colored curves) in the top Ta_2O_5 AR layers for the proposed bilayer absorbers-based RGB reflective color filters.

It is worth noting that the AR layer thickness d_2 equals to the one-eighth wavelength optical thickness of λ_0 for the designed green color filter, which is much different from the regular quarter-wave optical thickness of λ_0 for the red and blue colors. Figure S3 shows the bottom and top reflection phase shifts in top Ta_2O_5 layers for the proposed RGB color filters. It can be seen that the bottom reflection phase shifts are close to 0 at the wavelengths of λ_0 = 600 nm for the blue color and λ_0 = 400 nm for the red color, while the bottom reflection phase shift is ~ 0.5π at λ_0 = 460 nm for the green color. All the top reflection phase shifts are equal to −π. In order to satisfy the AR resonance condition, the propagation phase shift should be π for blue and red colors, and 0.5π for the green color, so that the net phase shifts are equal to a multiple of 2π. Therefore, d_2 should be fixed at $\frac{\lambda_0}{4n_2}$ for blue and red colors and $\frac{\lambda_0}{8n_2}$ for the green color, respectively.

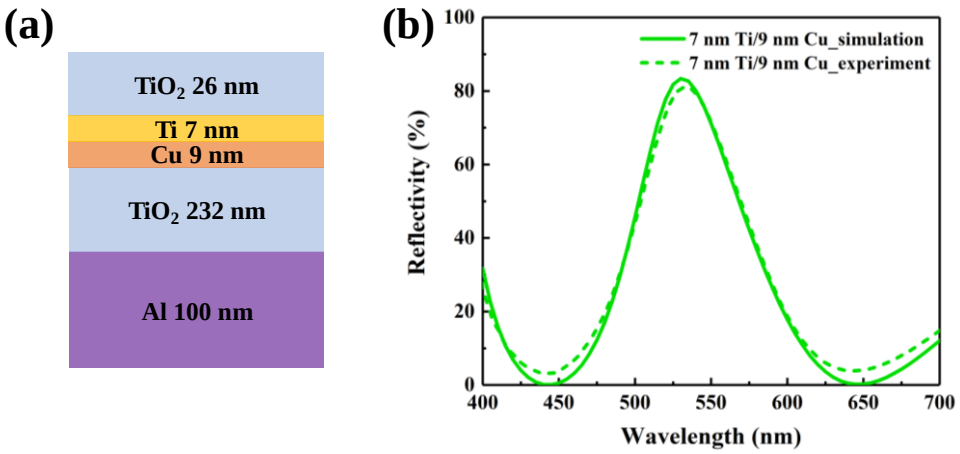

Figure S4. (a) A schematic diagram of a high-purity green color filter based on the Ti/Cu bilayer absorber. The lossless TiO_2 is applied for the dielectric layer and the AR layer. (b) The simulated and measured reflection spectra of the designed green color filter in (a), which both exhibit the maximum reflectivity exceeding 80%.

The relatively low reflection intensities of the proposed RGB color filters in Figure 2e resulted from the lossy property of Ta_2O_5 can be further improved by using a lossless dielectric material, such as TiO_2. According to the presented design principle, a kind of high-purity green reflective color filter adopting TiO_2 as the AR layer and the dielectric layer is designed as illustrated in Figure S4a. In this device, A bilayer film comprised of 7 nm Ti and 9 nm Cu is employed as the absorber layer. Obviously, a reflection peak at the wavelength of 532 nm with the reflectivity surpassing 80% appears in both the simulated and measured reflection spectra shown in Figure S4b. Besides, the device exhibits very low reflectivity in two undesired wavelength ranges of 400 ~ 500 nm and 600 ~ 700 nm, resulting in very high color purity. The calculated color coordinates (simulation (0.296, 0.596) and experiment (0.292, 0.587)) are very close to the standard Green (0.3, 0.6) utilized in liquid crystal displays (LCDs).

3. The RGB color filters with improved color purity by using different bilayer absorbers

CIE (x, y) coordinates	Red	Green	Blue
lossy medium #1	**(0.636, 0.360)**	**(0.346, 0.564)**	**(0.210, 0.088)**
lossy medium #2	**(0.537, 0.315)**	**(0.360, 0.553)**	**(0.157, 0.092)**
bilayer_simulation	**(0.640, 0.330)**	**(0.303, 0.600)**	**(0.151, 0.062)**
bilayer_experiment	**(0.620, 0.313)**	**(0.307, 0.592)**	**(0.153, 0.062)**
Standard color	**(0.640, 0.330)**	**(0.300, 0.600)**	**(0.150, 0.060)**

Table S1. The detailed 1931 CIE (x, y) coordinates in Figure 2f. The color coordinates of standard RGB colors utilized in liquid crystal displays (LCDs) are also displayed.

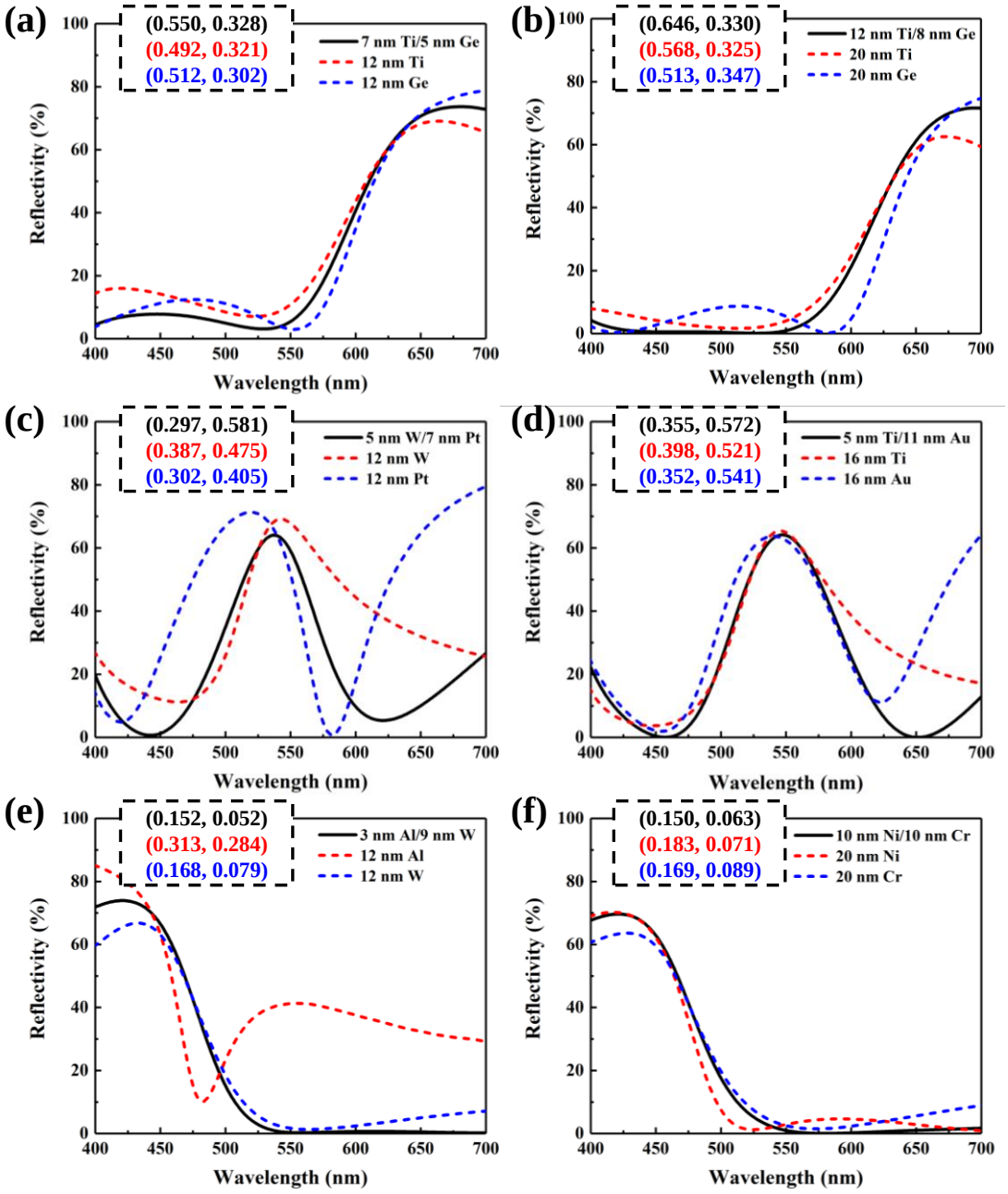

Figure S5. Comparison of the simulated reflection spectra of red (a, b), green (c, d) and blue (e, f) color filters based on suitable bilayer absorbers (black solid curves), single lossy medium absorbers (red dashed curves correspond to lossy medium #1 and blue dashed curves correspond to lossy medium #2) in the case of the other two absorber layer thicknesses. Their chromaticity coordinates calculated from the simulated spectra in the CIE 1931 color space are shown in the dotted boxes.

We also studied the possibility of using effective absorbing medium to improve the color purity of RGB reflective color filters in the case of the other two absorber

layer thicknesses (d = 12 and 20 nm for red and blue colors; d = 12 and 16 nm for green colors). Figure S5 shows the simulated reflection spectra for RGB color filters using single lossy media and bilayer films as the absorber layers. Obviously, optical absorptions in the wavelength range of non-target colors (500 ~ 700 nm for blue color filters, 400 ~ 600 nm for red color filters, 400 ~ 500 nm and 600 ~ 700 nm for green color filters) are significantly enhanced by using suitable bilayer absorbers for all the color filters. As a result, RGB color filters based on ultrathin bilayer absorbers show higher color purity than those employing single lossy medium absorbers, which can be further confirmed by comparing their color coordinates displayed in the dotted boxes. All the complex refractive indices of the materials used for our simulations are obtained from ellipsometry measurements as depicted in Figure S6.

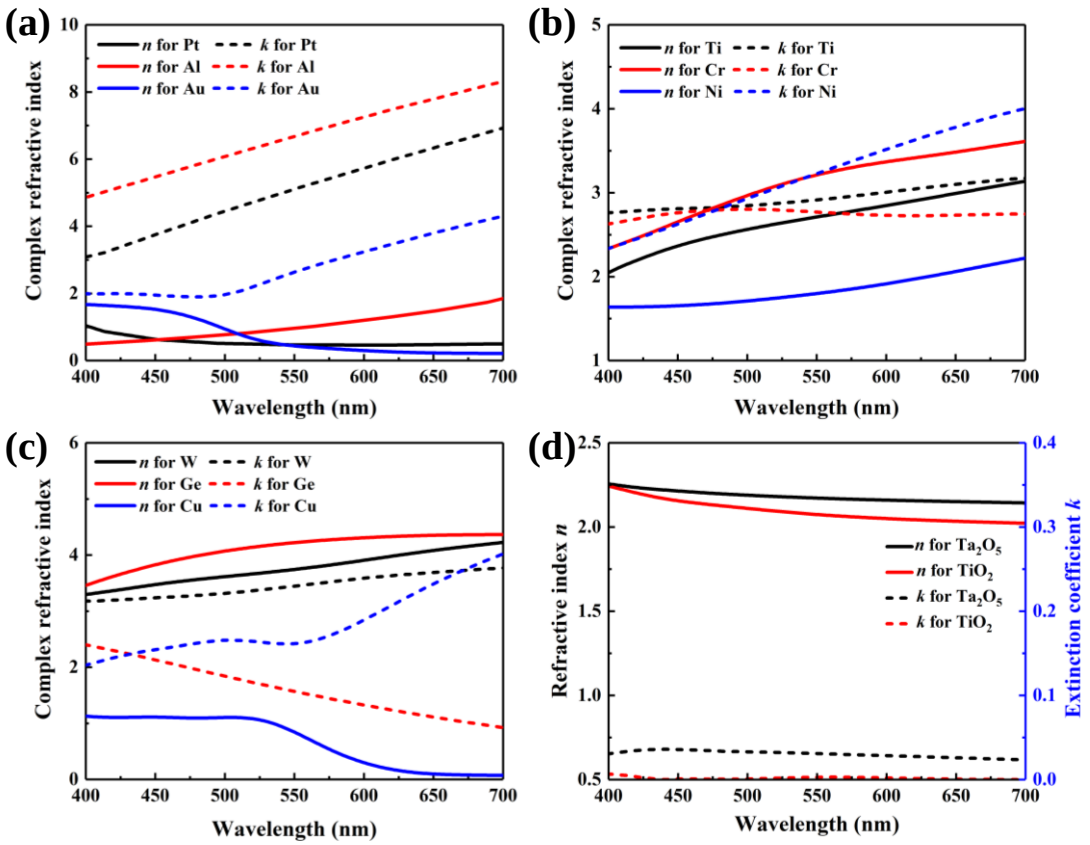

Figure S6. (a)-(d) The complex refractive indices of lossy materials and dielectric materials that are used for the calculations. The refractive indices (n) and extinction coefficients (k) are obtained using a spectroscopic ellipsometer (M-2000, J. A. Woollam) and are displayed with solid and dashed lines, respectively.

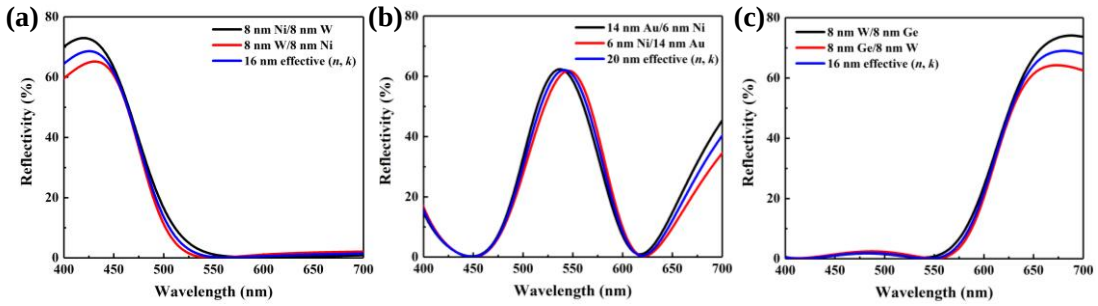

Figure S7. Comparison of the simulated reflection spectra of (a) blue, (b) green and (c) red color filters employing different absorbing medium. All black curves in (a-c) correspond to the ultrathin bilayer absorbers for high-purity RGB color filters discussed in the main text. All red curves correspond to the ultrathin bilayer absorbers after exchanging the positions of lossy medium #1 and lossy medium #2. All blue curves correspond to the effective absorbing media with the calculated effective complex refractive indices (*n*, *k*). The structural parameters of other layers are fixed for all three colors.

In order to verify the applicability of effective medium theory in our design concept, we compared the reflection spectra of RGB color filters employing the proposed ultrathin bilayer absorbers in Figure 2, the bilayer absorbers after exchanging the positions of lossy medium #1 and lossy medium #2, and the corresponding effective absorbing media with the calculated effective indices (*n*, *k*), as shown in Figure S7. For all the RGB color filters, their optical responses are basically consistent, including high reflectivity in the wavelength range of the target colors and high absorption of undesired wavelengths when using three kinds of absorber media mentioned above. The slight deviation of resonance wavelengths and reflection intensities in their spectra is mainly due to the difference of reflection phase shifts occurring at bilayer absorber/Ta_2O_5 interfaces. Therefore, the effective absorbing medium theory can be applied to explain the improved color purity of our designed structures.

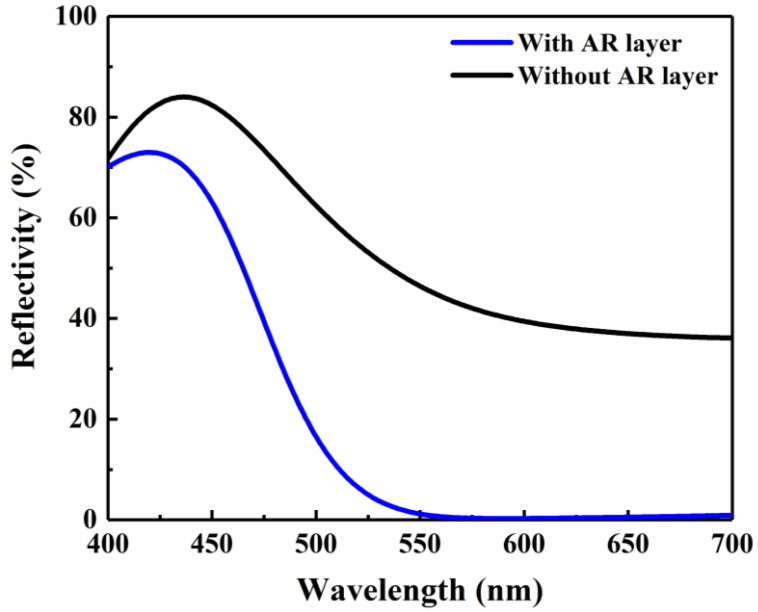

Figure S8. Spectra comparisons of the designed blue color filter with and without the top Ta_2O_5 AR layer, indicating that the top Ta_2O_5 AR layer can greatly reduce the broadband reflection outside the blue color range.

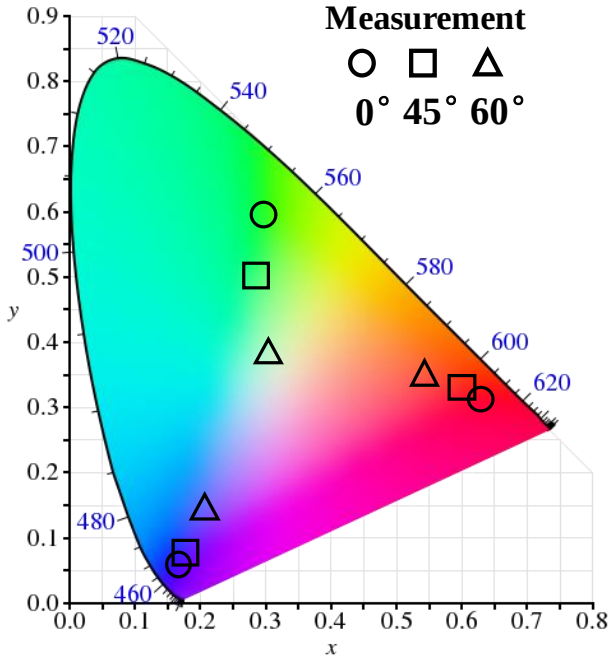

Figure S9. Visualization of color change with the incident angle on the CIE 1931 chromaticity diagram.

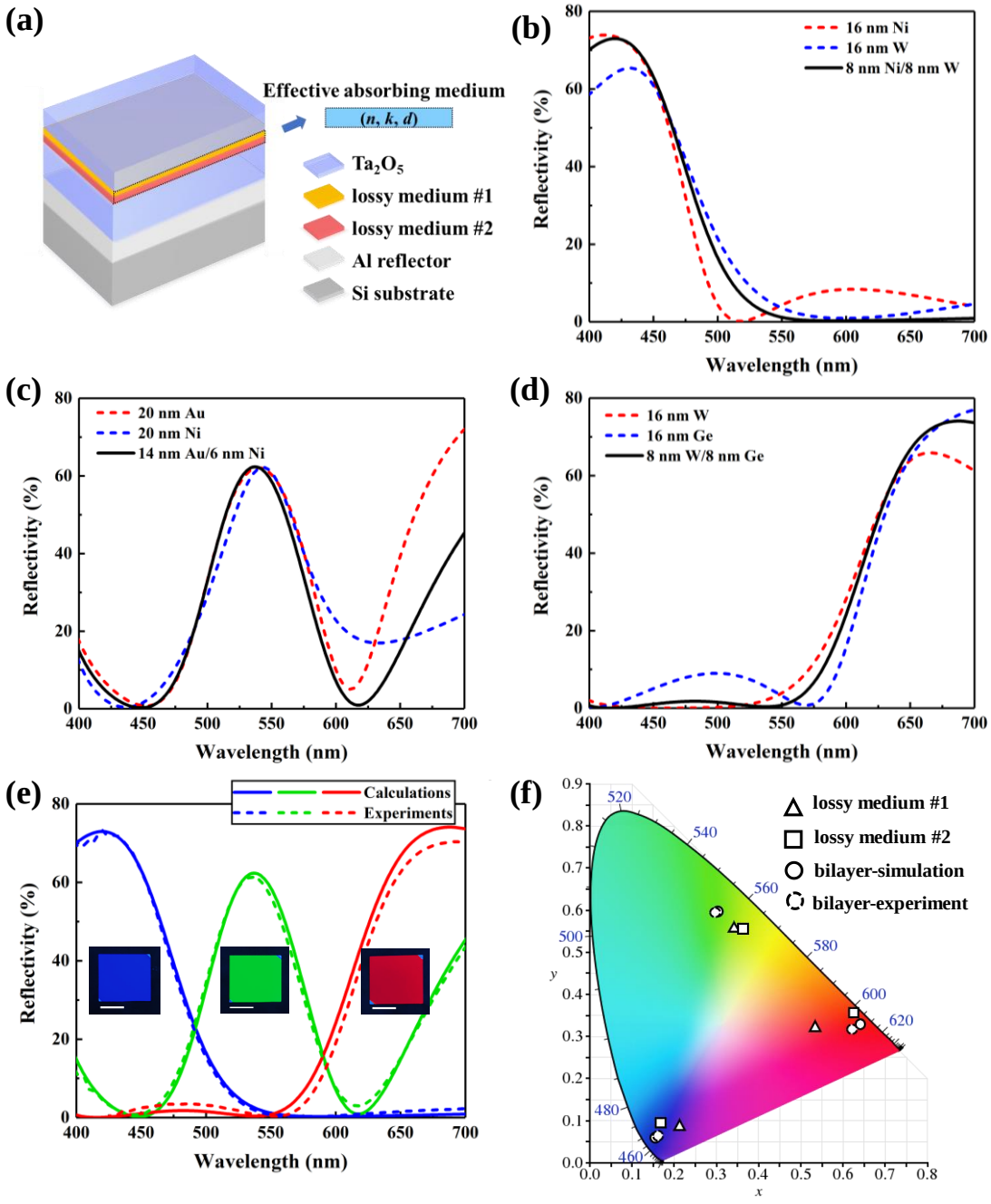

Figure 2. (a) A schematic view of the proposed high-color-purity RGB reflective color filters using bilayer absorbers. Two ultrathin lossy films (lossy medium #1 and lossy medium #2) can be regarded as an effective absorbing medium with the complex refractive index (n, k) and the total thickness d. (b-d) Comparison of the simulated reflection spectra of RGB color filters employing single lossy medium #1, lossy medium #2 and the corresponding bilayer as the absorber layer. (e) The simulated and measured reflection spectra of the proposed RGB color filters based on bilayer absorbers at

normal incidence. Insets show the optical images of fabricated RGB devices on silicon substrates (Scale bars: 1.0 cm). (f) The calculated chromaticity coordinates corresponding to all the reflection spectra shown in (b-e) in the CIE 1931 chromaticity diagram.

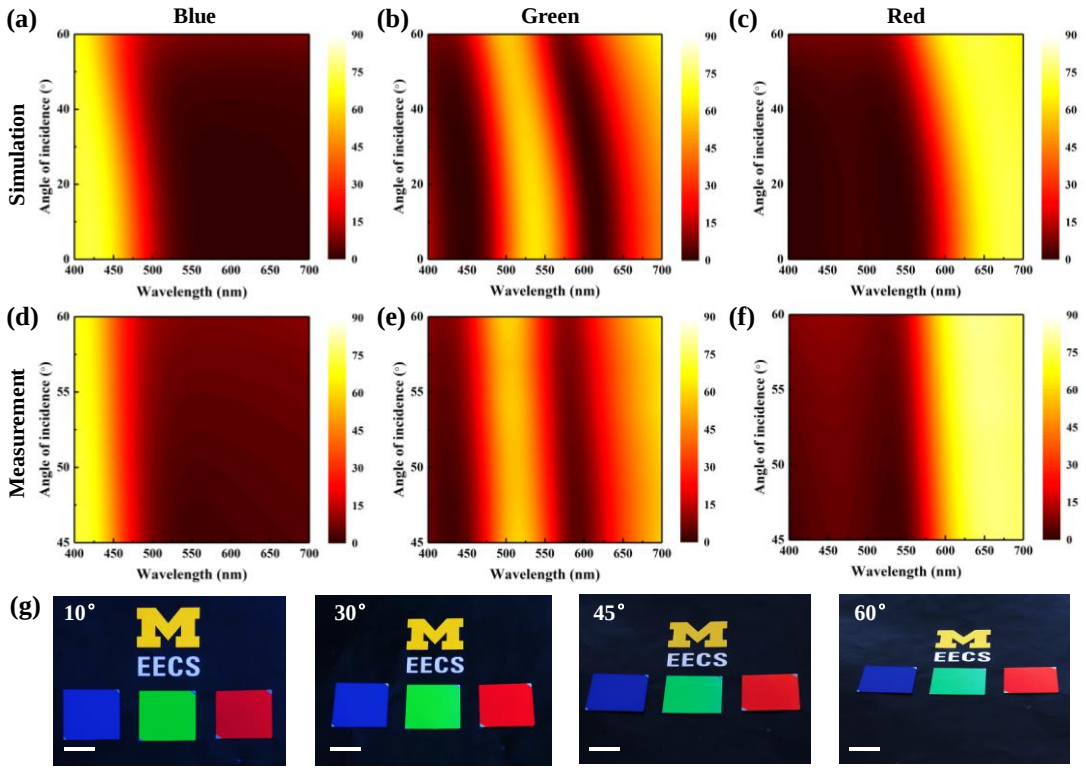

Figure 4. (a)-(c) The simulated and (d)-(f) measured angle-resolved reflection spectra of the proposed RGB reflective colors based on bilayer absorbers under unpolarized light incidence. (g) Photographic images of the fabricated samples taken at oblique incidence of 10°, 30°, 45° and 60°. The scale bars are 1.0 cm.